Permeability estimation from 2D image analysis and experimental data

Lorena A. B. Figueiredo*, Roseane M. Misságia, Marco A. R. de Ceia, Nathaly L. Archilha and Irineu A. de Lima Neto
North Fluminense State University, Brazil (UENF/LENEP)

This paper was prepared for presentation during the 14th International Congress of the Brazilian Geophysical Society held in Rio de Janeiro, Brazil, August 3-6, 2015.

Abstract

This article describes an approach to evaluate specific geometric properties measured in carbonate and sandstone from outcrop rocks. Carbonate exhibits a complex pore system with a broad pore size range, thus requiring special techniques to characterize such heterogeneous porous. Conversely, sandstone typically exhibits a regular distribution and pore size that result in a more homogeneous pore system, when compared to carbonate. The main goal of this work was using mercury porosimetry technique to identify the pore system of these rock types, and estimate the permeability (k) by Kozeny-Carman correlation using gas porosity (ϕ) and tortuosity (τ), which was determined by resistivity measure in laboratory, and form factor (fps) by Digital Image Analysis (DIA).

Introduction

Permeability has a great importance to petroleum geoscientists, although it is not easy to be estimated, due to the wide variety texture, porous system and characteristics of each reservoir. In this scope, it is essential identify parameters influencing permeability. Mercury porosimetry is a well-known technique used for describe the porous system, where pores can be investigated between 500 μm and 3.5 nm. Furthermore, this technique provides other important information, as the pore size distribution, porosity and hysteresis (Giesche, 2006).
In this work, mercury porosimetry technique was applied to ten outcrop samples (see Tab.1) to determine the pore size distribution, and the dominant pore size (DomSize) parameter from DIA, according to Weger (2009). From these results, permeability was estimated according to Kozeny – Carman theory, tortuosity was calculated by formation factor and gas porosity, and factor form from Digital Image Analysis (DIA). Thereafter, permeability estimates were compared to measured permeability.
In this work, one of the main goals of studying outcrop rocks is apply it to predict permeability of similar rock types.

Database

In this study, five carbonates and three sandstones extracted from USA outcrops were used. This carbonates pertain to following formation: Three as Edward Plateau (Edward Yellow, Edward white and Desert Pink), one as Thornton Formation (Silurian Dolomite), one as Valders Stone & Marble formation (Wisconsin). Sandstones samples were extracted from Kipton formation (Berea), Tennessee Formation (Crab Orchard), and Utah formation (Nugget). Table 1 lists the mineral composition obtained from X - Ray Diffraction and Rietveld method, in addition to classification of carbonates and sandstones outcrop rocks. In this study, all the following measurements were performed in the LENEP's laboratory: gas porosity (ϕ), gas permeability (Kg), mercury injection capillary pressure, X- Ray diffraction and electrical resistivity needed to determine tortuosity (τ) and cementation factor (m), seeTab.1.

Method

The Washburn equation is the basic calculation in mercury porosimetry and clearly provides a simple and convenient relationship between applied pressure and pore size (Léon, 1998).

$$\Delta P = \frac{2\,\gamma\cos\theta}{r}; \quad (1)$$

where γ is the surface tension of mercury, $\mathbf{r}$ the corresponding pore throat size and $\boldsymbol{\theta}$ the contact angle between the solid and mercury.
Generally the pore shape is quite different to the cylinder pore assumption; which can lead to major differences between analyzed and actual pore form.
In these experiments, the pressure limit applied by equipments in the porous material was 60.000 psi.

Pore size distribution

The pore size distribution is determined from mercury intrusion into pores as function of the applied pressure using Eq.1 (Léon, 1998). The volume of mercury penetration for each pressure is the difference between the respective cumulative intrusion volumes (Webb, 2001), as pressure increase, mercury is penetrated into the small pore throat.
There are many classifications for pore size system, i.e. according to Machado et al., (2012) micropores porous < 0.5 μm, mesopores between 0.5 μm and 5 μm and macropores >5 μm .
In addition to, note that in carbonate reservoir commonly more than 50% of the pore system are micropores (Yu, 2014).

Dominant Pore Size

Weger (2009) determined dominant pore size (DomSize) as the upper boundary of pore sizes of which 50% of the porosity on a thin section is composed. This parameter provides an indication of the pore-size range that dominates the sample. In this study, this parameter is applied only to carbonates samples and varies between 7.66 - 49.68 μm (see Tab.2).

Resistivity Formation Factor, Cementation factor and tortuosity

Electrical resistivity is the measure of the material ability to resist to the electric current. In 1942, Archie experimentally that the resistivity of a rock completely saturated with a conductive fluid, R_o, is related to the resistivity of the conductive fluid, R_w (Eq. 2).

$$R_{0=} FRF * R_w; \quad (2)$$

where FRF is the formation resistivity factor, as Eq. 3.

$$FRF = \phi^{-m}; \quad (3)$$

Here, "m" represents the slope of linear trend of $FRF x \phi$. Archie (1942) stated that m vary according to the degree of cementation of the rock, which it was estimated 1.3 for unconsolidated sands and ranged between 1.8 and 2.0 for cemented sandstones.
Tortuosity is defined as the ratio of the actual or effective length of a flow path to the length of a porous medium, and It varies according to the geometry of the pores, Φ and FRF, as shown Eq. 4, (Latour, 1995).

$$FRF * \phi = \tau; \quad (4)$$

Specific Surface Area

Specific surface area per unit pore volume is the internal surface area per volume, where the surface area A_s for n capillary tubes is $n(2\pi rL)$ and the pore volume is $n(\pi r^2 L)$ (Eq.5).

$$S_{Vp} = \frac{A_s}{V_P} = \frac{n(2\pi rL)}{n(\pi r^2 L)} = \frac{2}{r}. \quad (5)$$

For a bundle of capillary tubes, the total area exposed A_t is equivalent to the internal surface area A_s, the grain volume V_{gr} is equal to equation 6.

$$A_c L(1-\phi); \quad (6)$$

where A_c the total cross- sectional area and L is Length (Tiab & Donaldson, 2011).
S_{vgr} is the specific surface area of a porous material or the total area exposed within the per space per unit of grain volume (Eq.7).

$$S_{vgr=} \frac{n(2\pi rL)}{A_c l(1-\Phi)} = \frac{2\pi nr}{A_c(1-\Phi)} = \frac{\pi nr^2}{A_c}\left(\frac{2}{r}\right); \quad (7)$$

Equations 5, 6 and 7 give:

$$S_{vgr} = S_{Vp}\left(\frac{\phi}{1-\phi}\right); \quad (8)$$

Hysteresis

Through mercury porosimetry technique, hysteresis is used to describe the failure of the extrusion curve to retrace the intrusion curve, at the same pressure on the two curves. The extrusion curve with no hysteresis will exactly retrace the intrusion curve, and with hysteresis will always have volume values greater than the intrusion curve at the same pressure (Webb, 2001), and it represents the amount of mercury contained in the pore system. If the pores were uniform, the intrusion and extrusion happen at the same pressure, but generally samples show varied of geometries (Giesche, 2006).

Permeability

Permeability is the ability of a rock to permit fluids to flow through the interconnected pores. Carbonates have a complex and heterogeneous pore system, which makes it difficult to estimate the permeability. Kozeny-Carman is one of the most popular and fundamental correlations to estimate permeability in rocks, which correlates permeability to porosity, tortuosity and specific surface area per unit grain volume (S_{vgr}). These are important properties that directly interfere in the fluid flow through the rock (Izadi, 2012). In this work, it was considered the circular pore to estimate permeability, Eq. 9 (Tiab & Donaldson, 2011).

$$k_e = \frac{\phi^3}{(1-\phi)^2}\left[\frac{1}{f_{ps}\tau S_{gvr}^2}\right]; \quad (9)$$

Therefore, to obtain more specific results of the Φ and S_{vgr} were determined for each pore throat ratios and more volume fraction, i.e, Φ, S_{vgr} has been established by the sum.
The factor form was determined in accordance with DIA that was calculated from Eq.10 (Tiab & Donaldson, 2011). In the Eq. 10 Lp is pore perimeter and A_P refers for area pore.

$$f_{ps} = \frac{Lp^2}{4*A_P}; \quad (10)$$

In this work, DIA was used to identify only mesoporous and macroporous. Consequently, to estimate the permeabilities has been used mesopores and macropores.
In addition to DIA, Yu (2014) concluded that if carbonates present more than 50% of microporosity permeability will correlate better with porosity when microporosity has been deducted from total porosity.
Another way to estimate the permeability is using Eq. 11 that describes the flow through porous homogeneous.

$$k_c = c\frac{\Phi^3}{S_{vgr}{}^2}; \quad (11)$$

where c is an empirical constant only depend of Φ (Eq.12) (Mortensen et al., 1998).

$$c = \left(4\cos\left(\frac{1}{3}\arccos\left(\Phi\frac{8^2}{\pi^3}-1\right)+\frac{4}{3}\pi\right)+4\right)^{-1}; \quad (12)$$

Results

Figure 1 shows the pore throat distribution of carbonates and sandstones according to the classification present in Fig.6. Note that the carbonate (EW) and sandstones (NU and CO) report only the presence of micro and mesoporous, while the others samples exhibit all kind of pores. In this experiment the smallest pore size, which can be filled with mercury, was limited by the maximum pressure achieved by the mercury porosimetry equipment (Gieschi, 2006).

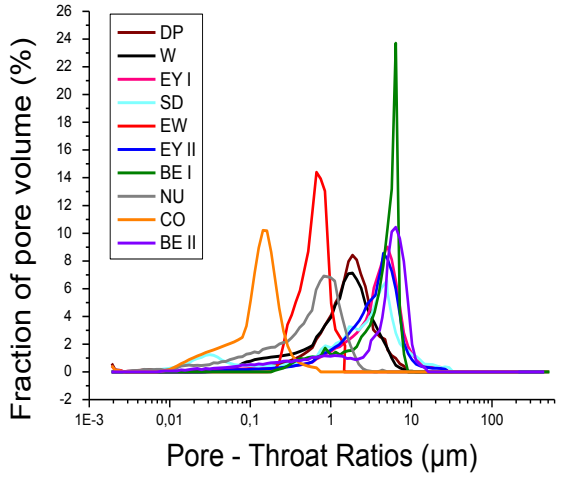

Figure 1 – Representation of pore size distribution of carbonate and sandstone samples in function of fraction of pore volume (%)

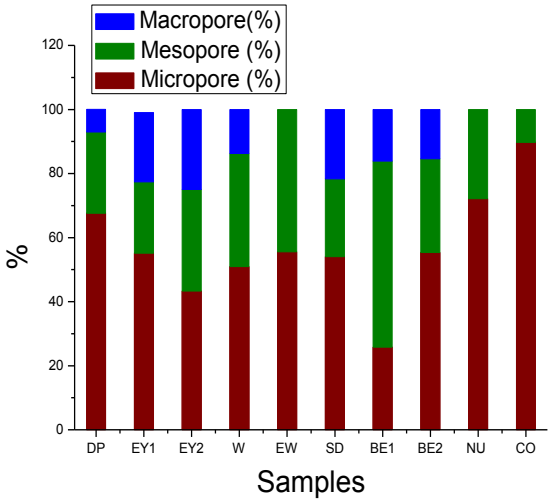

Figure 2 - Represents porous classification for carbonate and sandstone samples

Figures 3 and 4 submit the behavior of the rocks as a function of the tortuosity. If the pores are cylindrical, intrusion and extrusion happen at the same pressure. However, some of samples exhibit different intrusion and extrusion processes. This occurrence can be correlated with estimate tortuosity values. Observe in Table 1 that samples (EY I, EY II, SD, NU, CO) shows higher values of tortuosity and larger differences between extrusion and intrusion processes. Form factor is another important geometric parameter, where an ideal spherical pore is 1. Observe that rocks with higher τ values show higher f_{ps} values, except dolomite that has a lower value (1.53). Note that the difference between extrusion and intrusion retains a certain amount of mercury in the pores.

Figures 5 and 6 exhibit a correlation between K_g (i.e. involving all pores), K_e and K_c (Involving macro and mesoporous). It is possible to observe the good adjustment coefficient between estimates permeability expressed by $R^2 = 0.844$ and $R^2 = 0.897$.

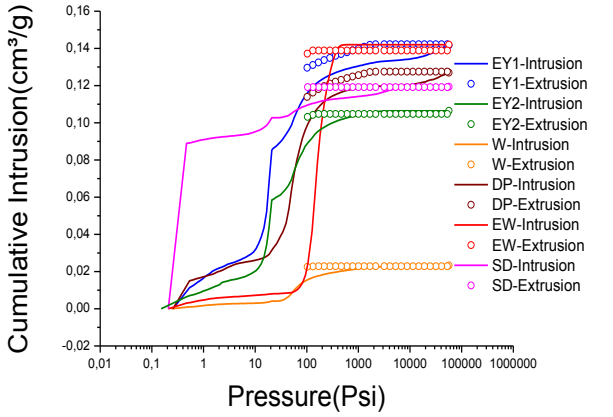

Figure 3 – Note the difference between extrusion and intrusion (carbonates) that retains a certain amount of mercury in the pores

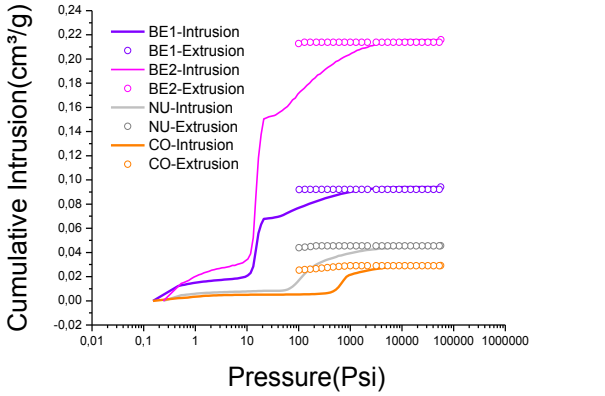

Figure 4 - Note the difference between extrusion and intrusion (sandstones) that retains a certain amount of mercury in the pores

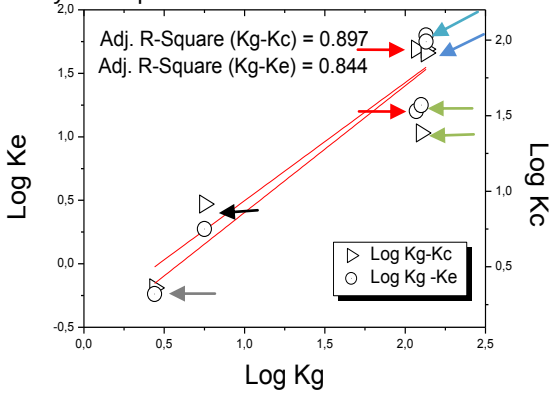

Figure 5 – Log K_g x Log K_e (carbonates). DP (red arrow), EY I and EY II (blue arrow), W (black arrow), SD (green arrow) and EW (gray arrow)

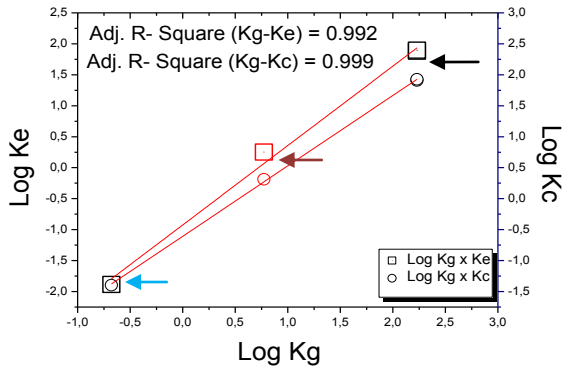

Figure 6 - Log K_g x Log K_e (sandstones). CO (blue arrow), NU (brown arrow) and BE I and BE II (black arrow)

Although K_e and K_c present close settings, K_e always has shown a lower value than K_c. Equations 9 and 11 clarify this event, since K_c depends on of the porosity (Φ) and specific surface area (S_{vgr}), conversely K_g depends on more than two variables as tortuosity (τ) and form factor (f_{ps}). Tortuosity directly influences the permeability, since it is defined as the way that the fluid flows. Therefore, tortuosity and cementation factors represent two critical parameters that significantly affect estimates of reservoir properties.

In this work, results demonstrated that tortuosity values of sandstones are inversely proportional to K_g and K_e estimates, Figures 5 and 6. This same analysis can be applied only to DP, W and EW carbonate samples, while EYI, EY II and SD carbonate samples show different behavior - high K_g and tortuosity values. Probably, these samples present high values of tortuosity because they were undergone diagenetic processes as dolomitization and cementation. These analyses can explain the classification of these samples, (Table 2).

Also, Table 1 shows that samples with porosity less than 12% present $m \leq 2$, while samples with higher porosity have $m > 2$, i.e., m increases when Φ increases.

Other factors can be involved in this analysis, as texture and mineralogical composition. The SD and W samples, for example, has dolomite as main mineral, while the others samples has calcite as main mineral, (Fig.9)

Despite a reasonable adjustment between these estimates of permeability, Figs 6 and 7 exhibit dispersion around points of crossplot. Also, in Table 1, observe that higher dispersions are always associated to higher percentage of micropores, (Fig.2).

Several (SD, EW, EY I, EY II) carbonate samples also had higher dispersion and more than 50% of microporosity, although (CO and NU) sandstones sample has showed great dispersion.

Madonna et al. (2013) showed that images generated by X-ray tomography, ultra - resolution (<1 microns) don´t contribute to the study of the permeability, since, for the transport of fluid flow flows through the macropores and the influence micropores is negligible.

In the DP sample is observed a relevant amount of micropores, but it didn´t show a higher dispersion as found in SD sample. Probably, these carbonates are manifesting a different behavior of porous system, since they may have suffered post-depositional alterations that modify the pore structure through diagenetic processes. This requires special analysis not yet performed in this study, for example, connectivity of pores and spatial information of the distribution of pore throat.

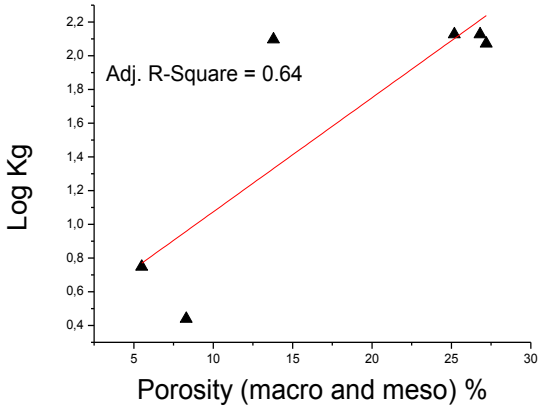

Figure 7 - Log Kg x $\phi_{(macro/meso)}$ for carbonate samples. If permeability increases, porosity also increases, as porosity is an important controlling factor on properties of fluid flow and transport in reservoir

Figure 7 shows a linear relation between K_g versus $\phi_{(macro/meso)}$ in which the obtained adjust coefficient - $R^2 = 0.64$, evidences that 64% of the K_g can be explained by macro and meso porosity.

Furthermore, multivariate linear regression (MLR) was applied to permeability, porosity, and 2D DIA parameter of the pore space, obtained from thin section, to enhancement the coefficient of determination R^2 (Fig.8). A 3D crossplot of DomSize and $\phi_{(meso\ and\ macro)}$ with K_g shows the link between the dominant pore size (DomSize), ϕ and K_g, when R^2 increases from 0.64 to 0.84. It means that these parameters account 84% of the K_g, expressing a strong relationship among pore space properties and a geometric parameter of the pore space.

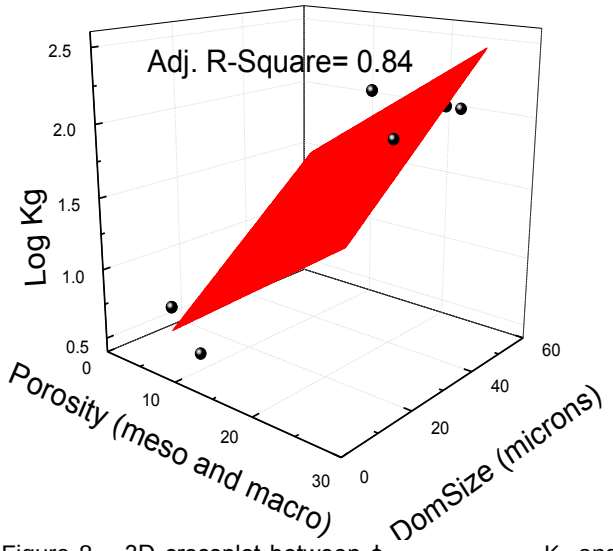

Figure 8 – 3D crossplot between $\phi_{(macro\ and\ meso)}$, K_g and DomSize (carbonates). Note an improvement when DomSize is included on statistic model demonstrating its importance to improve K_g

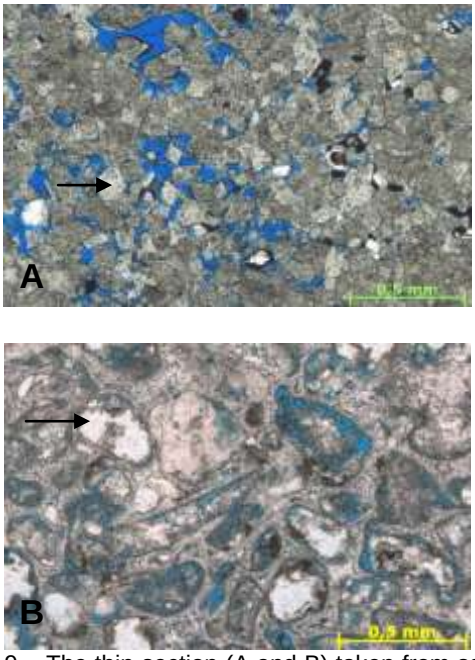

Figure 9 – The thin-section (A and B) taken from samples (SD and EY, respectively). The thin-section A shows a dolomite grains (arrow) and B shows the cemented grainstone with calcite grains (arrow)

Conclusions

- Although the mercury porosimetry equipment was limited to 60,000 psi, the experiments were successful to fill out even the smallest pores; henceforth it was possible to evaluate pore size distribution for each of the samples and implement these results in permeability estimates.
- The two ways to estimate the permeability proposed in this paper represent gas permeability, even using different parameters. Highlight the porosity (meso and macro) because it is a parameter that directly influences permeability.
- Hysteresis shows that carbonate rocks with higher values of tortuosity present larger differences between extrusion and intrusion, i.e. larger amount of mercury was retained in the pore. The same conclusion can be applied to form factor for some rocks, it is important to highlight the dolomite that sample presents higher value of tortuosity and lower form factor between carbonates rocks, what can be explained to diagenetic process or by the methodology used for determined form factor.
- Despite a reasonable adjustment between these estimates of permeability and gas permeability, these measures exhibit higher dispersions values are always associated to higher percentage of micropores.
- A combination of porosity (macro and meso) and DomSize explains more than 84% of the gas permeability, demonstrating it ability as controlling factors of permeability.

Acknowledgments

We thank UENF/LENEP for facilities provided to perform this work, ANP-PRH-226 for financial support and scholarship.

References

Archie, G.E., 1942. **The electrical resistivity log as an aid in determining some reservoir characteristics**. Trans. AIME 146, 54–62.

Dunham, Robert J. **Classification of carbonate rocks**
Folk, Robert L. **Petrology of sedimentary rocks**. Hemphill Publishing Company, 1980.

Gieschi, Herbert. **Mercury porosimetry: a general (practical) overview**. Particle & particle systems characterization, v. 23, n. 1, p. 9-19, 2006.

Leon, C. (1998). **New perspective in mercury porosimetry.** Advances in Colloid and Interface Science, 76-77, 341-372.

Machado, Vinicius et al. **Carbonate Petrophysics in Wells Drilled with Oil-Based Mud.** Petrophysics -SPWLA-Journal of Formation Evaluation and Reservoir Description, v. 53, n. 4, p. 285, 2012.

Madonna, Claudio et al. **Synchrotron-based X-ray tomographic microscopy for rock physics investigations**. Geophysics, v. 78, n. 1, p. D53-D64, 2013.

Mortensen, Jeanette; Engstrom, F.; Lind, Ida. **The relation among porosity, permeability, and specific surface of chalk from the Gorm field, Danish North Sea.** SPE Reservoir Evaluation and Engineering, v. 1, p. 245-251, 1998.

Tiab, Djebbar; Donaldson, Erle C. **Petrophysics: theory and practice of measuring reservoir rock and fluid transport properties.** Gulf professional publishing, 2011.

Webb, Paul A. **An introduction to the physical characterization of materials by mercury intrusion porosimetry with emphasis on reduction and presentation of experimental data.** Micromeritics Instrument Corp, Norcross, Georgia, 2001.

Weger, Ralf J. et al. **Quantification of pore structure and its effect on sonic velocity and permeability in carbonates**. AAPG bulletin, v. 93, n. 10, p. 1297-1317, 2009.

Yu, Yibing et al. **Quantitative Effect of Microporosity on Permeability in Carbonate Reservoirs**. In: International Petroleum Technology Conference. International Petroleum Technology Conference, 2014.

Table 1 - Results and information for samples selected for this study.

Rocks	Samples	K_g (gas permeability)	K_e (estimate permeability using eq.9)	K_c (estimate permeability using eq.11)	tortuosity (τ)	gas porosity(ϕ)	Porosity (macro and meso) (%)	cementation factor (m)	Form factor (F_{ps})	Formation Resistivity Factor (FRF)	σ K_gxK_e *	σ K_gxK_c *
Carbonates	DP (Desert Pink)	118.00	48.57	33.91	3.41	31.00	27.2	2.04	1.78	11.00	0.59	0.19
	EY I (Edward Yellow)	134.00	49.47	108.00	9.2	27.60	25.18	2.86	2.00	41.05	0.63	0.26
	EY II (Edward Yellow)	134.00	45.60	98.84	9.2	27.60	26.8	2.86	2.00	41.05	0.66	0.00
	W (Wisconsin)	5.60	2.96	5.60	6.27	6.80	5.5	1.75	1.50	112.00	0.47	0.23
	EW (Edward White)	2.75	0.65	2.11	9.71	11.70	8.3	2.05	2.00	82.89	0.76	0.70
	SD (Silurian Dolomite)	125.00	10.80	37.40	15.39	19.90	13.,8	2.6	1.53	85.98	0.91	0.53
Sandstones	BE I (Berea)	170.00	77.09	80.63	3.84	19.30	18.5	1.81	1.75	20.24	0.55	0.50
	BE II (Berea)	170.00	80.00	84.62	3.84	19.30	15.4	1.81	1.75	20.24	0.53	0.65
	NU(Nugget)	5.93	1.78	2.05	5.14	10.30	5.8	1.75	1.82	49.00	0.70	0.65
	CO(Crab orchard)	0.21	0.01	0.04	8.7	8.40	0.08	1.87	2.00	103.60	0.95	0.81

* Dispersion between results of Kg and Ke/ Kg and Kc

Table 2- Results and information for samples selected for this study.

Rocks	Samples	Textural Classification **	Mineralogical Composition***	Dom size (Microns)
Carbonates	DP (Desert Pink)	crystalline carbonate	Calcite 99.8% Quartz 0.2%	20.4
	EY I (Edward Yellow)	cemented grainstone	Calcite 99.7% Quartz 0.3%	42.62
	EY II (Edward Yellow)			
	W (Wisconsin)	crystalline carbonate	dolomite 83% quartz 16.3% calcite 0.7%	7.66
	EW (Edward White)	grainstone/packstone	Calcite 99.7 % quartz 0.12% Sylvite 0.18%	9.88
	SD (Silurian Dolomite)	Dolomite	dolomite 98% quartz 1.6% alumina 0.4%	49.68
Sandstones	BE I (Berea)	Subarcóseo	quartz 94% alumina 4.05% , Iron oxide 1.05 % calcite 0.9%	-
	BE II (Berea)			-
	NU(Nugget)	quartz-sandstone	quartz 96.7% mica 3.3%	-
	CO(Crab orchard)	Subarcóseo	quartz 93% mica 6.05% feldspar 0.95%	-

**Dunham´s Carbonate Rock texture classification (1962) and Folk´s Sandstone Rock Classification (1980). ***Mineralogical composition (DRX and Rietveld method).